Modelling cell motility with the evolving surface finite element method

C. Venkataraman
Joint work with C. Elliott and B. Stinner

Warwick Mathematics Institute WMI

June 11, 2012

Directed motion of cells is central to many biological processes, e.g., cancer metastasis, wound healing and immune responses.

./../Movies_webpage/Keratocyte_experimental.mp4

Persistent migration of a fish keratocyte

./../Movies_webpage/pseudopod.mov

Dictyostelium chemotaxis [King and Insall, 2009]

Modelling chemotaxis with ESFEM [Elliott, Stinner, and Venkataraman, 2012]

- Modelling
- Discretisation
- Simulations

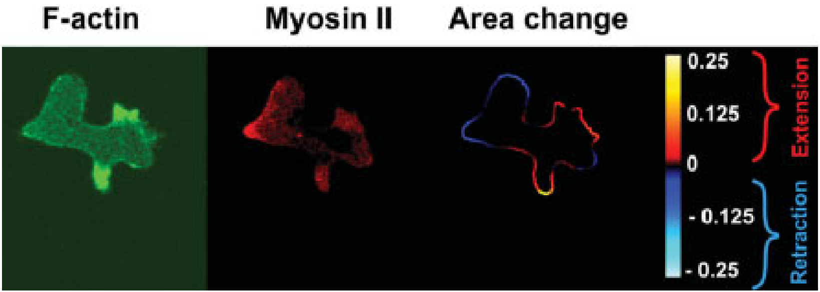

Figure: Cell polarisation and movement [Bosgraaf, van Haastert, and Bretschneider, 2009]

(plausible) Model

- Polarisation and gradient sensing: PDE posed on a continuously evolving surface.
- Movement: Surface evolution law coupled to surface PDE.

Model: Coupled surface RDS surface evolution law

(Turing) Reaction-diffusion system (RDS) on an evolving surface [Dziuk and Elliott, 2007]

$$\partial^{\bullet}_{\boldsymbol{V}} \boldsymbol{a} + \boldsymbol{a} \nabla_{\Gamma(t)} \cdot \boldsymbol{V} - \boldsymbol{D} \Delta_{\Gamma(t)} \boldsymbol{a} = \boldsymbol{f}(\boldsymbol{a}) \text{ on } \Gamma(t), t > 0, \qquad \boldsymbol{a}(\cdot, 0) = \boldsymbol{a}^0(\cdot) \quad \text{on } \Gamma(0),$$

where $\boldsymbol{D}$ is a diagonal matrix of positive diffusion coefficients, $\boldsymbol{a}^0$ is a bounded vector valued function, $\boldsymbol{V}$ is the material velocity of the surface and the material derivative with respect to $\boldsymbol{V}$ is

$$\partial^{\bullet}_{\boldsymbol{V}} \boldsymbol{a} := \partial_t \boldsymbol{a} + \boldsymbol{V} \cdot \nabla \boldsymbol{a}$$

Evolution law

$$\boldsymbol{V} = \Bigg(\underbrace{\boldsymbol{K}_p \cdot \boldsymbol{a}}_{\text{Protrusion/Retraction}} - \underbrace{k_s H}_{\text{MCF (resistance to stretching)}} \underbrace{+ k_b \left(\Delta_\Gamma H + H \left| \nabla_\Gamma \boldsymbol{\nu} \right|^2 - \frac{1}{2} H^3 \right)}_{\text{WF (resistance to bending)}} + \underbrace{\lambda}_{\text{Volume conservation}} \Bigg) \boldsymbol{\nu}.$$

For closed curves as $\left| \nabla_\Gamma \boldsymbol{\nu} \right|^2 = H^2$:

$$\boldsymbol{V} \cdot \boldsymbol{\nu} |_{d=2} = \boldsymbol{K}_p \cdot \boldsymbol{a} - k_s H + k_b \left(\Delta_\Gamma H + \frac{1}{2} H^3 \right) + \lambda.$$

Numerical methods

Geometric evolution equations [Deckelnick, Dziuk, and Elliott, 2005]

- Level set [Droske and Rumpf, 2004; Sethian, 1999]
- Phase field [Du, Liu, and Wang, 2004; Lowengrub, Rätz, and Voigt, 2009]
- Parametric [Bänsch, Morin, and Nochetto, 2005; Barrett, Garcke, and Nürnberg, 2008; Bonito, Nochetto, and Sebastian Pauletti, 2010; Dziuk, 2008; Elliott and Stinner, 2010]

Surface PDEs

- Diffuse interface [Elliott, Stinner, Styles, and Welford, 2011; Rätz and Voigt, 2006]
- Closest point [Macdonald and Ruuth, 2009; Ruuth and Merriman, 2008]
- Surface finite elements [Dziuk and Elliott, 2007], finite volumes [Lenz, Nemadjieu, and Rumpf, 2008]

Main advantage of SFEM is efficiency.

Cons: Harder to include bulk phenomena, No topological change.

Surface finite elements [Dziuk, 1990]

Approximate the surface (curve) Γ with a polyhedral (polygonal) surface Γ_h:

$$\Gamma_h = \cup_{T_h \in \mathscr{T}} T_h .$$

Surface finite element space:

$$\mathbb{V}^m := \{\chi_h \in \mathrm{H}^1(\Gamma_h^m) : \chi_h|_{T_h} \text{ is quadratic (linear)}\}.$$

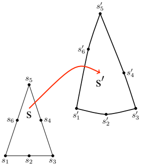

Isoparametric quadratic surface finite elements are (possibly) curved images of a linear reference element under a quadratic map.

Use of isoparametric quadratic surface finite elements in $3d$ motivated by the need to approximate $\nabla_\Gamma \boldsymbol{\nu}$.

$O(h^{\ell-1})$ convergence of the Weingarten map (for a given smooth surface) in L_2 was shown in [Heine].

Discretisation

Schemes based on variational form of the identity

$$H\boldsymbol{\nu} = -\Delta_\Gamma \boldsymbol{x}.$$

In $3D$ approximation of the shape operator based on the identity:

$$\int_\Gamma \nabla_\Gamma \boldsymbol{\nu} \cdot \Phi = -\int_\Gamma \boldsymbol{\nu} \cdot (\nabla_\Gamma \cdot \Phi) + \int_\Gamma H\boldsymbol{\nu} \cdot \Phi\boldsymbol{\nu}.$$

Weak formulation

$$\int_{\Gamma(t)} \left(\partial_t \boldsymbol{x} \cdot \boldsymbol{\nu}\chi + k_b \nabla_{\Gamma(t)} H \cdot \nabla_{\Gamma(t)}\chi - k_b H \left|\boldsymbol{\nu}\right|^2 \chi + \frac{1}{2} k_b H^3 \chi + k_s H\right) = \int_{\Gamma(t)} \left(\lambda\chi + \boldsymbol{k}_p \cdot \boldsymbol{a}\chi\right)$$

$$\int_{\Gamma(t)} \left(H\boldsymbol{\nu} \cdot \boldsymbol{\chi} - \nabla_{\Gamma(t)} \boldsymbol{x} : \nabla_{\Gamma(t)} \boldsymbol{\chi}\right) = 0, \quad \forall \chi \in \mathrm{H}^1(\Gamma(t)), \boldsymbol{\chi} \in \mathrm{H}^1(\Gamma(t))^d$$

Discretisation of the evolution law by parameterising Γ_h^{n+1} over Γ_h^n, based on the scheme of [Barrett, Garcke, and Nürnberg, 2008]. Induces a tangential velocity that results in good mesh-properties.
Surface densities treated explicitly.

Discrete curve evolution

Given $\boldsymbol{X}_h^n \in (\mathbb{V}^n)^2$, $H_h^n \in \mathbb{V}^n$ and $\boldsymbol{a}_h^n \in (\mathbb{V}^n)^m$, find $\boldsymbol{X}_h^{n+1} \in (\mathbb{V}^n)^2$, $H_h^{n+1} \in \mathbb{V}^n$ such that

$$\int_{\Gamma_h^n} \left(\frac{1}{\tau} \left(\boldsymbol{X}_h^{n+1} - \boldsymbol{X}_h^n \right) \boldsymbol{\nu}_h^n \chi_h + k_b \nabla_{\Gamma_h^n} H_h^{n+1} \cdot \nabla_{\Gamma_h^n} \chi_h - \frac{1}{2} k_b \left(H_h^n \right)^2 H_h^{n+1} \chi_h + k_s H_h^{n+1} \chi_h \right) = \int_{\Gamma_h^n} \left(\lambda^{n+1} + \boldsymbol{k}_p \cdot \boldsymbol{a}_h^m \right) \chi_h$$

$$\int_{\Gamma_h^n} \left(H_h^{n+1} \boldsymbol{\nu}_h^n \cdot \boldsymbol{\chi}_h - \nabla_{\Gamma_h^n} \boldsymbol{X}_h^{n+1} : \nabla_{\Gamma_h^n} \boldsymbol{\chi}_h \right) = 0,$$

for all $\chi_h \in \mathbb{V}^n$, $\boldsymbol{\chi}_h \in (\mathbb{V}^n)^2$.

Discrete surface evolution

Given $\boldsymbol{X}_h^n \in (\mathbb{V}_2^n)^3$, $H_h^n \in \mathbb{V}_2^n$ and $\boldsymbol{a}_h^n \in (\mathbb{V}_2^n)^m$, first find $\boldsymbol{Q}_h^n \in (\mathbb{V}_2^n)^{3\times 3}$ such that

$$\int_{\Gamma_h^n} \boldsymbol{Q}_h^n \Phi_h = \int_{\Gamma_h^n} \left(H_h^n \boldsymbol{\nu}_h^n \Phi_h \boldsymbol{\nu}_h^n - \boldsymbol{\nu}_h^n \nabla_{\Gamma_h^n} \cdot \Phi_h \right) \quad \forall \Phi_h \in (\mathbb{V}_2^n)^{3\times 3},$$

then find $\boldsymbol{X}_h^{n+1} \in (\mathbb{V}_2^n)^3$, $H_h^{n+1} \in \mathbb{V}_2^n$ such that

$$\int_{\Gamma_h^n} \Bigg(\frac{1}{\tau} \left(\boldsymbol{X}_h^{n+1} - \boldsymbol{X}_h^n \right) \boldsymbol{\nu}_h^n \chi_h + k_b \nabla_{\Gamma_h^n} H_h^{n+1} \cdot \nabla_{\Gamma_h^n} \chi_h + k_b \left(\frac{1}{2} (H_h^n)^2 - \left| \boldsymbol{Q}_h^n \right|^2 \right) H_h^{n+1} \chi_h$$
$$+ k_s H_h^{n+1} \chi_h \Bigg) = \int_{\Gamma_h^n} \left(\lambda^{n+1} \chi_h + \boldsymbol{k}_p \cdot \boldsymbol{a}_h^m \chi_h \right)$$
$$\int_{\Gamma_h^n} \left(H_h^{n+1} \boldsymbol{\nu}_h^n \cdot \boldsymbol{\chi}_h - \nabla_{\Gamma_h^n} \boldsymbol{X}_h^{n+1} : \nabla_{\Gamma_h^n} \boldsymbol{\chi}_h \right) = 0,$$

for all $\chi_h \in \mathbb{V}_2^n$, $\boldsymbol{\chi}_h \in (\mathbb{V}_2^n)^3$.

Enforcing the constraint

Linear system

Given data at time t^m we have the linear system

$$\begin{bmatrix} (\boldsymbol{N}^m)^T & \boldsymbol{C}^m \\ -\boldsymbol{A}^m & \boldsymbol{N}^m \end{bmatrix} \begin{bmatrix} \boldsymbol{x}_h^{m+1} \\ H_h^{m+1} \end{bmatrix} = \begin{bmatrix} \lambda^{m+1}\boldsymbol{b}_h^m + \boldsymbol{f}_h^m \\ 0 \end{bmatrix}.$$

Solve linear system with right hand sides $\boldsymbol{f}_h$ and $\boldsymbol{b}_h$, then determine λ^{m+1} via a Newton method [Bonito, Nochetto, and Sebastian Pauletti, 2010] such that volume is conserved. Newton method yields $\boldsymbol{x}_h^{m+1}$ and H_h^{m+1}.

Cost two solves per timestep (iterative solver) for a direct solver only one matrix factorisation per timestep is needed.

RDS approximation

- Discretisation of the RDS via an ALE-ESFEM [Dziuk and Elliott, 2007].
- (Lagrangian) ESFEM nodes moved with material velocity $\boldsymbol{V} = v\boldsymbol{\nu}$.
- In our case nodal movement includes artificial tangential velocity $\boldsymbol{V}_{ALE} := \partial_t \boldsymbol{X} = v\boldsymbol{\nu} + \boldsymbol{T}$.

We have

$$\begin{aligned}\partial^{\bullet}_{\boldsymbol{V}} a + a\nabla_\Gamma \cdot \boldsymbol{V} &= \partial_t a + \boldsymbol{V} \cdot \nabla a + a\nabla_\Gamma \cdot \boldsymbol{V} \\ &= \partial_t a + \boldsymbol{V}_{ALE} \cdot \nabla a + a\nabla_\Gamma \cdot \boldsymbol{V}_{ALE} - \nabla_\Gamma \cdot (a\boldsymbol{T}) \\ &= \partial^{\bullet}_{\boldsymbol{V}_{ALE}} a + a\nabla_\Gamma \cdot \boldsymbol{V}_{ALE} - \nabla_\Gamma \cdot (a\boldsymbol{T})\end{aligned}$$

Thus an equivalent strong formulation of the RDS reads

$$\partial^{\bullet}_{\boldsymbol{V}_{ALE}} \boldsymbol{a} + \boldsymbol{a}\nabla_{\Gamma(t)} \cdot \boldsymbol{V}_{ALE} - \nabla_\Gamma \cdot (a\boldsymbol{T}) - \boldsymbol{D}\Delta_{\Gamma(t)}\boldsymbol{a} = \boldsymbol{f}(\boldsymbol{a})$$

RDS weak formulation

Leibniz formula [Dziuk and Elliott, 2007]

$$\frac{\mathrm{d}}{\mathrm{d}t}\langle a_h, \chi_h\rangle_{\Gamma_h} = \left\langle \partial^{\bullet}_{\boldsymbol{V}_{ALE}}(a_h), \chi_h\right\rangle_{\Gamma_h} + \left\langle a_h, \partial^{\bullet}_{\boldsymbol{V}_{ALE}}\chi_h\right\rangle_{\Gamma_h} + \langle a_h, \chi_h \nabla_\Gamma \cdot \boldsymbol{V}_{ALE}\rangle_{\Gamma_h} \tag{1}$$

Thus the transport property of the basis functions (w.r.t the ALE-velocity) gives

Weak formulation semidiscrete

$$\frac{\mathrm{d}}{\mathrm{d}t}\langle (a_h)_i, \chi_h\rangle_{\Gamma_h} - \left\langle \nabla_{\Gamma_h} \cdot ((a_h)_i \boldsymbol{T}_h), \chi_h\right\rangle_{\Gamma_h} + \left\langle D_i(\nabla_{\Gamma_h}(a_h)_i), \nabla_{\Gamma_h}\chi_h\right\rangle_{\Gamma_h} = \langle f_i(\boldsymbol{a}_h), \chi_h\rangle_{\Gamma_h}$$

for all $\chi_h \in \mathbb{V}(t)$.

- The ALE-velocity plays the role of an (extra) advective flux in the RDS.

RDS discrete scheme

Discrete scheme

We employ an IMEX method where the reaction terms are treated explicitly and diffusion implicitly. Given Γ_h^{m+1} find $\boldsymbol{a}_h^{m+1} \in \mathbb{V}^{m+1}$ such that for $i = 1, \ldots, I$:

$$\int_{\Gamma_h^{m+1}} \left(\frac{(a_h)_i^{m+1}}{\tau} - \nabla_{\Gamma_h^m} \cdot ((a_h)_i \boldsymbol{T}_h^{m+1}) + D_i \nabla_{\Gamma_h^{m+1}} (a_h)_i^{m+1} \nabla_{\Gamma_h^{m+1}} \right) \chi_h^{m+1} = \int_{\Gamma_h^m} \frac{(a_h)_i^m \chi_h^m}{\tau} + f_i(\boldsymbol{a}_h^m) \chi_h^m .$$

The timestep needed for the surface update is sufficiently small that explicit treatment of the nonlinear reaction kinetics necessitates no further timestep restriction.

Implementation in ALBERTA [Schmidt and Siebert, 2005].

- Provides Isoparametric surface finite elements.
- Mesh adaptivity through newest vertex bisection (only employed for computations in $3d$)

Linear systems solved using UMFPACK [Davis, 2004].
Visualisation with PARAVIEW.

Tangential redistribution

./../Movies_webpage/equidistribution.avi

Persistent migration

Related work:

- [Keren, Pincus, Allen, Barnhart, Marriott, Mogilner, and Theriot, 2008] experimental study with simple mathematical model neglecting details of cell shape
- [Shao, Rappel, and Levine, 2010] Coupled surface evolution law bulk RDS, phase field numerics
- [Ziebert, Swaminathan, and Aranson, 2011] Coupled surface evolution law bulk equation for orientation of actin filaments, phase field numerics

Schnakenberg model

$$\partial^{\bullet}_{\boldsymbol{V}} a_1 + a_1 \nabla_{\Gamma(t)} \cdot \boldsymbol{V} - D_1 \Delta_\Gamma a_1 = \gamma \left(k_1 - a_1 + a_1^2 a_2 \right),$$
$$\partial^{\bullet}_{\boldsymbol{V}} a_2 + a_2 \nabla_{\Gamma(t)} \cdot \boldsymbol{V} - D_2 \Delta_\Gamma a_2 = \gamma \left(k_2 - a_1^2 a_2 \right), \quad \text{on } \Gamma(t), t > 0,$$
$$\boldsymbol{a}(\cdot, 0) = \boldsymbol{a}^0(\cdot) \quad \text{on } \Gamma_0.$$

- activator (a_1) promotes retraction of the cell membrane ($(k_p)_1 < 0$).
- Substrate (a_2) promotes protrusion of the cell membrane ($(k_p)_2 > 0$).

Persistent migration

Experiments show cells move at a constant speed with fixed shape. Positive relationship between aspect ratio and cell speed [Keren, Pincus, Allen, Barnhart, Marriott, Mogilner, and Theriot, 2008].

./../Movies_webpage/keratocyte_curve.avi

./../Movies_webpage/keratocyte_surface.avi

Pseudopod driven migration

Related work:

- [Neilson, Mackenzie, Webb, and Insall, 2011] Coupled surface RDS surface evolution law, (2d) level set and SFEM numerics
- Lots of others e.g., [Hecht, Skoge, Charest, Ben-Jacob, Firtel, Loomis, Levine, and Rappel, 2011; Jilkine and Edelstein-Keshet, 2011]

Meinhardt model

Extension of the [Meinhardt, 1999] model. Local activator (a) antagonised by a local inhibitor (c) and a global (rapidly distributed) inhibitor (b) [Amarasinghe, Aylwin, Madhavan, and Pettitt, 2011; Neilson, Mackenzie, Webb, and Insall, 2011].

$$\partial^{\bullet}_{\boldsymbol{V}} a + a \nabla_{\Gamma(t)} \cdot \boldsymbol{V} - D_a \Delta_\Gamma a = \gamma \left(\frac{r_a s (a^2/b + b_a)}{(s_c + c)(1 + s_a a^2)} - r_a a \right),$$

$$b = \frac{1}{|\Gamma|} \int_\Gamma a,$$

$$\partial^{\bullet}_{\boldsymbol{V}} c + c \nabla_{\Gamma(t)} \cdot \boldsymbol{V} - D_c \Delta_\Gamma c = \gamma (b_c c - r_c a),$$

where $s(\boldsymbol{x}, t)$ models random fluctuations due to underlying noise and the stochastic chemotactic signal. (See B. Stinner's talk for details)

- Spatial patterning due to local activation-global inhibition. Temporal patterning due to the local inhibitor.
- Signals amplified due to autocatalysis.
- Coupling to evolution law only through protrusive force proportional to activator (a) density.

We assume the chemotactic signal and underlying noise are OU processes [Neilson, Mackenzie, Webb, and Insall, 2011]. Approximated via the Euler-Maruyama method.

./../Movies_webpage/signal_change.avi

Response to a changing signal

Pseudopod driven migration in 3*d*

./../Movies_webpage/3dcell.avi

Migration of an unstimulated cell in 3*d*

Migration in heterogeneous media

./../Movies_webpage/Neutrophil_Rogers1950s.mp4

Experiment of Rogers [1952], neutrophil chasing a bacteria in a sea of obstacles (corpuscles)

./../Movies_webpage/obstacle_mcf.avi

Simulation based on simple phenomenological model

Summary

- Coupled surface evolution - surface RDS model capable of replicating aspects of cell behaviour observed during chemotaxis.
- Computational method capable of dealing with general surface PDE coupled to a surface evolution law consisting of surface tension and elastic flow in the presence of constraints.
- Movement in complex enviroments.
- Movement of 3D cells.

Future work

Crawling on a substrate

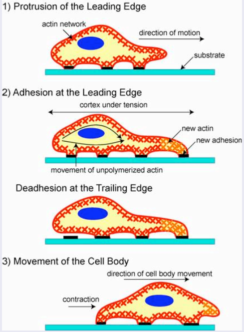

./../movies/curved.avi

Analysis

Well posedness (curves), Self-intersection
Numerical analysis:

- PDEs on evolving surfaces [Dziuk and Elliott, 2012; Lubich, Mansour, and Venkataraman]
- Geometric evolution laws [Deckelnick and Dziuk, 2010]

Thank You

D.P. Amarasinghe, A. Aylwin, P. Madhavan, and C. Pettitt. Biomembranes report. MASDOC, RSG, 2011.

E. Bänsch, P. Morin, and R.H. Nochetto. A finite element method for surface diffusion: the parametric case. *Journal of Computational Physics*, 203(1):321–343, 2005.

J.W. Barrett, H. Garcke, and R. Nürnberg. Parametric approximation of willmore flow and related geometric evolution equations. *SIAM Journal on Scientific Computing*, 31:225, 2008.

A. Bonito, R.H. Nochetto, and M. Sebastian Pauletti. Parametric fem for geometric biomembranes. *Journal of Computational Physics*, 229(9):3171–3188, 2010.

L. Bosgraaf, P.J.M. van Haastert, and T. Bretschneider. Analysis of cell movement by simultaneous quantification of local membrane displacement and fluorescent intensities using quimp2. *Cell motility and the cytoskeleton*, 66 (3):156–165, 2009.

Timothy A. Davis. Algorithm 832: Umfpack v4.3—an unsymmetric-pattern multifrontal method. *ACM Trans. Math. Softw.*, 30:196–199, June 2004. ISSN 0098-3500. doi: http://doi.acm.org/10.1145/992200.992206. URL http://doi.acm.org/10.1145/992200.992206.

K. Deckelnick and G. Dziuk. Error analysis for the elastic flow of parametrized curves. *Mathematics of Computation*, 78(266):645, 2010.

K. Deckelnick, G. Dziuk, and C.M. Elliott. Computation of geometric partial differential equations and mean curvature flow. *Acta Numerica*, 14:139–232, 2005. ISSN 0962-4929.

M. Droske and M. Rumpf. A level set formulation for willmore flow. *Interfaces and Free Boundaries*, 6(3):361–378, 2004.

Q. Du, C. Liu, and X. Wang. A phase field approach in the numerical study of the elastic bending energy for vesicle membranes. *Journal of Computational Physics*, 198(2):450–468, 2004.

G. Dziuk. An algorithm for evolutionary surfaces. *Numerische Mathematik*, 58(1):603–611, 1990.

G. Dziuk. Computational parametric willmore flow. *Numerische Mathematik*, 111(1):55–80, 2008.

G. Dziuk and C.M. Elliott. Finite elements on evolving surfaces. *IMA journal of numerical analysis*, 27(2):262, 2007.

G. Dziuk and C.M. Elliott. L2-estimates for the evolving surface finite element method. *Math Comp (to appear)*, 2012.

Charles M. Elliott, Björn Stinner, and Chandrasekhar Venkataraman. Modelling cell motility and chemotaxis with evolving surface finite elements. *Journal of The Royal Society Interface*, 2012. doi: 10.1098/rsif.2012.0276. URL http://rsif.royalsocietypublishing.org/content/early/2012/05/29/rsif.2012.0276.abstract.

C.M. Elliott and B. Stinner. Modeling and computation of two phase geometric biomembranes using surface finite elements. *Journal of Computational Physics*, 229(18):6585–6612, 2010.

C.M. Elliott, B. Stinner, V. Styles, and R. Welford. Numerical computation of advection and diffusion on evolving diffuse interfaces. *IMA Journal of Numerical Analysis*, 31(3):786–812, 2011.

I. Hecht, M.L. Skoge, P.G. Charest, E. Ben-Jacob, R.A. Firtel, W.F. Loomis, H. Levine, and W.J. Rappel. Activated membrane patches guide chemotactic cell motility. *PLoS Computational Biology*, 7(6):e1002044, 2011.

CJ Heine. Isoparametric finite element approximation of curvature on hypersurfaces. Preprint.

A. Jilkine and L. Edelstein-Keshet. A comparison of mathematical models for polarization of single eukaryotic cells in response to guided cues. *PLoS Computational Biology*, 7(4), 2011.

K. Keren, Z. Pincus, G.M. Allen, E.L. Barnhart, G. Marriott, A. Mogilner, and J.A. Theriot. Mechanism of shape determination in motile cells. *Nature*, 453(7194):475–480, 2008.

Jason S. King and Robert H. Insall. Chemotaxis: finding the way forward with dictyostelium. *Trends in Cell Biology*, 19(10):523 – 530, 2009. ISSN 0962-8924. doi: DOI:10.1016/j.tcb.2009.07.004. URL `http://www.sciencedirect.com/science/article/pii/S0962892409001548`.

M. Lenz, S.F. Nemadjieu, and M. Rumpf. Finite volume method on moving surfaces. Technical report, Citeseer, 2008.

J.S. Lowengrub, A. Rätz, and A. Voigt. Phase-field modeling of the dynamics of multicomponent vesicles: Spinodal decomposition, coarsening, budding, and fission. *Physical Review E*, 79(3):031926, 2009.

Ch. Lubich, D. Mansour, and C. Venkataraman. Backward difference time discretization of parabolic differential equations on evolving surfaces. Submitted.

C.B. Macdonald and S.J. Ruuth. The implicit closest point method for the numerical solution of partial differential equations on surfaces. *SIAM J. Sci. Comput*, 31(6):4330–4350, 2009.

H. Meinhardt. Orientation of chemotactic cells and growth cones: models and mechanisms. *Journal of Cell Science*, 112(17):2867, 1999.

M.P. Neilson, J. Mackenzie, S. Webb, and R.H. Insall. Modelling cell movement and chemotaxis pseudopod based feedback. *SIAM Journal on Scientific Computing*, 33(3), 2011.

A. Rätz and A. Voigt. Pde's on surfaces—a diffuse interface approach. *Communications in Mathematical Sciences*, 4(3):575–590, 2006.

S.J. Ruuth and B. Merriman. A simple embedding method for solving partial differential equations on surfaces. *Journal of Computational Physics*, 227(3):1943–1961, 2008.

A. Schmidt and K.G. Siebert. *Design of adaptive finite element software: The finite element toolbox ALBERTA*. Springer Verlag, 2005.

J.A. Sethian. *Level set methods and fast marching methods: evolving interfaces in computational geometry, fluid mechanics, computer vision, and materials science*. Number 3. Cambridge Univ Pr, 1999.

D. Shao, W.J. Rappel, and H. Levine. Computational model for cell morphodynamics. *Physical review letters*, 105 (10):108104, 2010.

F. Ziebert, S. Swaminathan, and I.S. Aranson. Model for self-polarization and motility of keratocyte fragments. *Journal of The Royal Society Interface*, 2011.